XII International Conference on Computational Plasticity. Fundamentals and Applications
COMPLAS XII
E. Oñate, D.R.J. Owen, D. Peric and B. Suárez (Eds)

IMPLEMENTATION OF A LODE ANGLE SENSITIVE YIELD CRITERION FOR NUMERICAL MODELLING OF DUCTILE MATERIALS IN THE LARGE STRAIN RANGE

T: COPPOLA[*], L. CORTESE[†] AND F. CAMPANELLI[†]

[*] Centro Sviluppo Materiali, V. di Castel Romano 100, 00128 Rome, Italy
e-mail: t.coppola@c-s-m.it, web page: http://www.c-s-m.it
[†] Mechanical and Aerospace Engineering Department, Sapienza - Università di Roma, via Eudossiana, 18, 00184 Rome, Italy
Email: luca.cortese@uniroma1.it; flavia.campanelli@uniroma1.it- Web page: http://www.uniroma1.it

Key words: Yield surface, Lode angle, Torsion, Steel, Large strain.

Abstract. Ductile metallic materials are usually mechanically characterized in the large strain range by means of conventional laboratory tests, namely tensile and torsion test. The identification of the elastic-plastic equivalent stress-strain relation is made by using the widely accepted *J2* hypothesis and isotropic behaviour, but results of dedicated tensile and torsion tests on different steel grades showed that it does not seem possible to identify a unique stress-strain curve, as expected on theoretical ground. Curves obtained from dissimilar tests, even though perfectly matching at small plastic strains, start differing significantly from medium strains. Starting from the experimental observations, a general yield surface has been developed based on a well established framework, including beside the *J2* invariant also the *J3* one. The new yield function has been coded inside a general purpose finite element code by means of dedicated user routines. Implications on the parameters identification and examples of the new yield surface application are discussed in the paper.

1 INTRODUCTION

To describe the evolution of the yield surface in ductile isotropic metals like steels, the most popular criterion is based on *J2* plasticity. According to this, yielding and flow stress are governed by the second deviatoric stress invariant only.
Limits of *J2*-plasticity are well-known since the works of Lode [1], Ros and Eichinger [2], Taylor and Quinney [3], who demonstrated that the model was not able to accurately reproduce all experimental evidences. Nevertheless, the correlation with experimental outcomes was found to be sufficiently good, in particular for the low-medium plastic range, so that the *J2*-plasticity, also thanks to its ease of calibration and implementation, has been widely employed for research purposes and industrial practice. The use of more comprehensive theories has been for a long time considered to add just more difficulties than benefits.

Nowadays, cold forming of materials or increasing demand for strain based design require the modeling of material behavior in the high plastic strain regime and an accurate description of stress and strain distribution at critical points, originated from complex loading conditions.

Moreover, also ductile damage accumulation strongly depends on the state of stress, so that plasticity issues cannot be neglected for a good assessment of ultimate resistance of materials. It is then no coincidence that, in recent years, attempts to overcome *J2*-plasticity drawbacks have come from the ductile damage community.

Several alternative plasticity models have been proposed. Starting from extensive experimental studies [5-7], Brunig [8] and Kuroda [9] have found out that a plasticity model involving the first stress invariant also allows a more accurate prediction of deformation, localization and fracture behaviors in pressure-sensitive materials.

The contribution to yielding and flow stress of the third deviatoric stress invariant (*J3*) has also been investigated, and the opportunity of including it in the yield function has been discussed by the way of theoretical considerations, experimental tests and micromechanical analyses [10-12]. For many materials, the introduction of a *J3* term in the yield function [13-14] seems to accommodate a systematic discrepancy between the Von Mises (i.e. *J2*) criterion and the experimental results. Plasticity models involving three stress invariants are put forth and experimentally validated in [15-17]. A systematic review of not-*J2* criteria, covering a wide range of different materials, is reported in [18].

Soil and rock materials have been systematically described [19-21] including the Lode stress parameter into the constitutive laws. For this purpose, a very general and robust formulation for the yield function has been proposed by Bigoni and Piccolroaz for geomaterials [21]. Such formulation has been customized in the present work to provide a method of differentiating between the Tresca and the Von Mises yield criteria. The new formulation has been applied to the plasticity modeling in the high strain regime of steels.

2 MATERIALS AND MECHANICAL TESTING

Three steels have been selected for mechanical testing: EN 10083 *33MnB5*, commonly used in automotive applications and API 5L *grade 52* and *65*, for pipeline construction. All steels are supplied in form of seamless pipes, with dimensions, overall mechanical properties and delivery state reported in table 1.

Table 1: Mechanical properties of investigated steels

	Delivery state	**Pipe dimension [mm]**		**Yield Stress [MPa]**	**Ultimate Stress [MPa]**	**Elongation at break [%]**
		diameter	**thickness**			
Grade 65	*quenched and relieved*	406	20	440	530	18
Grade 52	*quenched and relieved*	168	5	395	565	33
33MnB5	*annealed*	65	8	455	615	15

The three steels can be regarded as fully isotropic due to the fact that all of them are supplied after the final high temperature heat treatment, which reset any deformation induced anisotropy due to the manufacturing process. Proof of isotropic behavior is also verified from tensile properties in longitudinal and tangential direction [22].

All tensile and torsion specimens were extracted in the pipe longitudinal direction, at mid thickness position. The dimensions have been defined according to the available thickness. Round section tensile test specimens have a gage diameter and length of 6x40 mm for steels *Grade 65* and *33MnB5* and 3x18mm for steel *Grade 52*. Torsion specimens have a gage diameter and length of 8x17mm for steel *Grade 65*, 5x10mm for steel *33MnB5* and 3.5x10mm for steel *Grade 52*.

Tension tests have been executed on a 100 kN servo-hydraulic MTS machine while torsion tests have been performed on a custom-made tension-torsion biaxial frame [23]. Continuous registration of axial displacement and force by an extensometer and a load cell during tensile tests allowed to obtain the true stress-true strain curves up to necking. The extended true stress-true strain curve beyond necking was characterized by means of an inverse calibration procedure [24-25], under the assumptions of *J2*-plasticity. Torque and rotation angle data, registered continuously during the torsion tests, have been used to determine true stress-true strain curves too: in this case, a direct calibration procedure is available [26] and *J2*-plasticity was assumed as well.

All tests were performed with at least two repetitions. In the following, the mean value is reported. Under the *J2* hypothesis, the two curves coming out from tensile and torsion tests should be coincident, while a large difference was obtained, as can be observed in Figures 1-3. It can be noticed that, except for steel *Grade 52*, the tensile and torsion curves are nearly coincident up to a plastic strain of about *0.15* which is equal or greater than the necking strain. After that point, the difference is becoming large, with torsion curves systematically lower than tension ones. It is so excluded any systematic error in the inverse calibration procedure used to determine the true stress-true strain curve after necking from tensile test. Moreover, if the extended curves were wrong, numerical simulation of tensile test using curves from torsion would match experimental results, while it was verified that this does not happen. For the sake of brevity outcomes of such verification are not reported here.

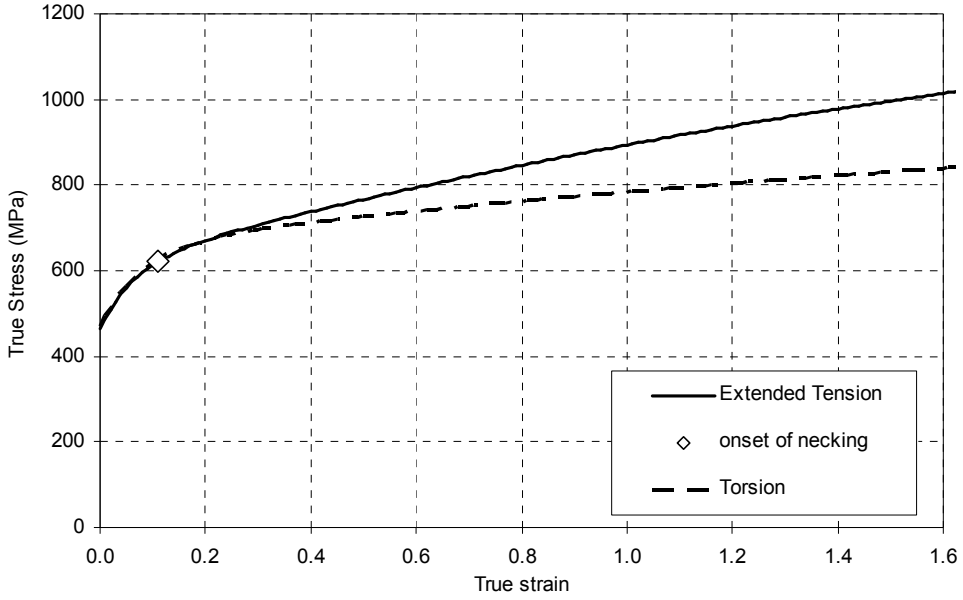

Figure 1: *Grade 65*: True stress-true strain curves from tension and torsion tests

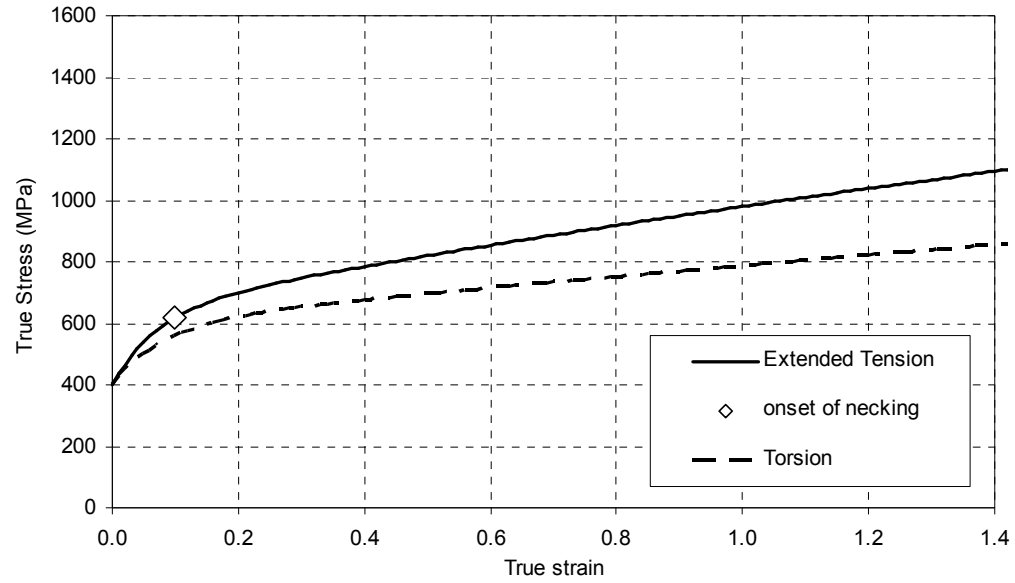

Figure 2: *Grade 52*: True stress-true strain curves from tension and torsion tests

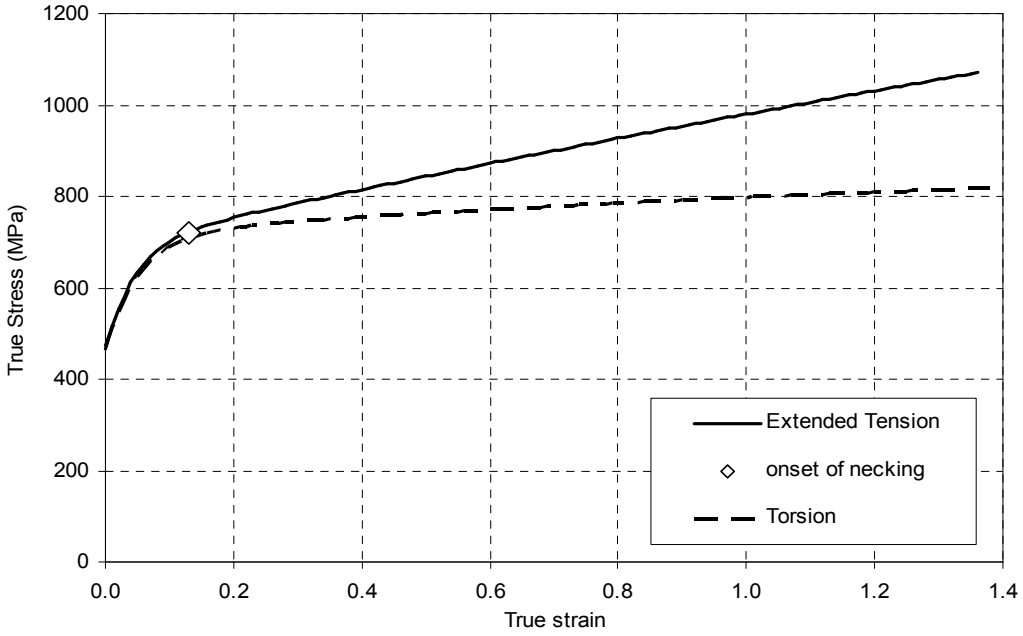

Figure 3: 33MnB5: True stress-true strain curves from tension and torsion tests

In order to account for this discrepancy, the hypothesis is that, at least at large strains, subsequent yielding is governed not only by the second deviatoric invariant stress (*J2*) but also by the Lode parameter, related to the third deviatoric invariant stress (*J3*). In other words, the section of the yielding surface in the deviatoric plane of the stress space is not a circle (von Mises criterion) but may be a generalized symmetric polygon.

3 A LODE ANGLE SENSITIVE YIELD CRITERION

The proposed criterion is valid under the assumptions of material homogeneity and isotropy, plastic incompressibility, isotropic hardening behavior, pressure insensitivity (i.e., no yielding occurs under hydrostatic tension or compression).

The yield function is a specialization of the unified yield function by Bigoni and Piccolroaz [21], which, in its formulation for pressure-insensitive materials, is reduced to:

$$F = \frac{q}{g(X)} - k \tag{1}$$

where $q = \sqrt{3J_2}$ is the equivalent Von Mises stress; *g(X)* is a function of the Lode parameter defined as $X = \frac{27}{2}\frac{J_3}{q^3}$ and $X \in [-1;1]$:

$$g(X) = \left[\cos\left(\beta\frac{\pi}{6} - \frac{1}{3}\arccos(\gamma X)\right)\right]^{-1} \tag{2}$$

Through the function *g(X)* it is possible to model the shape of the yield surface deviatoric section [21]. Three material parameters are needed:

- *k*, which characterizes the isotropic hardening effect and depends on the accumulated plastic strain;
- $\beta \in [0;2]$ which governs the so-called strength-differential phenomenon;
- $\gamma \in [0;1)$ which rules the polygonal shape to the yield surface and its corners rounding.

Function (1) reduces to classical yielding function for specific values of β and γ: Von Mises criterion is obtained for $\beta=1$ and $\gamma=0$; Tresca criterion is obtained for $\beta=1$ and $\gamma \to 1$. The modified plasticity model proposed is derived from (1), under the following developments. As first, the material constant *k* is obtained from (1) by imposing the condition for the uniaxial state of stress. In this case $X=1$, $q = \sigma_Y$ and we obtain:

$$k = \frac{\sigma_Y}{g(X=1)} \tag{3}$$

Next, according to the observed experimental behavior, the material is assumed to obey the Von Mises criterion for low plastic deformations; beyond the threshold value (ε_{th}), subsequent yield surface is distorted in the deviatoric plane. Such a distortion is governed by the accumulation of plastic strain, so that the new yield surface can be described by:

$$q\frac{g(X=1)}{g(X)} - \sigma_Y = 0 \tag{4}$$

with:

$$\beta = \begin{cases} 1 & \varepsilon^p \le \varepsilon_{th} \\ \beta(\varepsilon^p) & \varepsilon^p > \varepsilon_{th} \end{cases} \tag{5}$$

$$\gamma = \begin{cases} 0 & \varepsilon^p \le \varepsilon_{th} \\ \gamma(\varepsilon^p) & \varepsilon^p > \varepsilon_{th} \end{cases} \tag{6}$$

The function (2) satisfies the convexity requirements also for variable parameters β , γ provided that functions (5) and (6) always satisfy the limits $\beta \in [0;2]$ and $\gamma \in [0;1)$. Note that for *X=1* (as in tensile stress state), eq. (4) reduces to the Von Mises criterion independently from the level of plastic deformation: this is consistent with the assumption that led to (3). Since γ is initially zero and must go towards 1, the yield surface section evolves to a polygonal shape with corners (Figure 4a). It will be shown in the next sections that the curves in Figures 1-3 diverge too much for the effect being caught by a variation of the yield function produced by the γ parameter alone. Concerning β, it follows that it should increase towards 2 to capture the experimental evidences; as a consequence of this parameter variation, the yield surface tends to lose its symmetry as shown (Figure 4b).

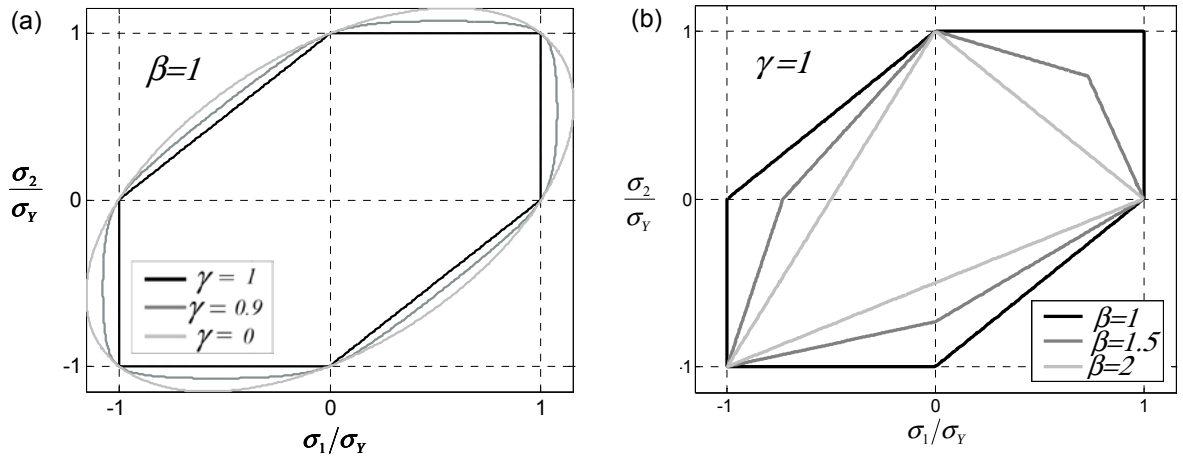

Figure 4: Yield surface, section with $\sigma_3 = 0$: (a) variation of γ at fix ed β ; (b) variation of β at fixed γ

For the functions (5) and (6) simple exponential laws are chosen to describe variation of β and γ with equivalent plastic strain:

$$\beta = \begin{cases} 1 & \varepsilon^p \le \varepsilon_{th} \\ 2 - \exp[-b(\varepsilon^p - \varepsilon_{th})] & \varepsilon^p > \varepsilon_{th} \end{cases} \tag{7}$$

$$\gamma = \begin{cases} 0 & \varepsilon^p \le \varepsilon_{th} \\ 1 - \exp[-a(\varepsilon^p - \varepsilon_{th})] & \varepsilon^p > \varepsilon_{th} \end{cases} \tag{8}$$

The parameters to be identified are so ε_{th} , a , b. Besides the yield function, a proper flow rule has to be postulated. Here, an associated flow rule is assumed:

$$d\varepsilon_{ij}^{p} = d\varepsilon^{p} \frac{dF(J_2, J_3)}{d\sigma_{ij}} \tag{9}$$

where $d\varepsilon^{p}$ is the equivalent plastic strain increment and $\frac{dF}{d\sigma_{ij}}$ are the derivatives of eq. (1) with respect to tensor stress components. As stated in [14], as far as pressure-sensitive materials concern, the flow rule is associative in the deviatoric plane only, in order to fulfill plastic incompressibility.

4 IMPLEMENTATION IN FINITE ELEMENT CODE

The implementation of the yield criterion in a Finite Element code requires the coding of the function *F* inequation (1) together with its derivatives in equation (9). The Finite Element code used is *Msc.Marc* which, through two specific user routines [28], allows this separately.

The function *F* doesn't require special mention. About derivatives (9), two schemes have been adopted: to write directly the (9) expanded starting from (1) or use a numerical scheme.

For the first case, it is easier to expand first the derivative of *F* respect to *q* and *g*:

$$\frac{\partial F}{\partial \sigma_{ij}} = \frac{q}{g}\left[\frac{1}{q}\frac{\partial q}{\partial \sigma_{ij}} - \frac{1}{g}\frac{\partial g}{\partial \sigma_{ij}}\right] \tag{10}$$

Next we can expand the derivatives of *q* and *g* respect to stress components:

$$\frac{\partial q}{\partial \sigma_{ij}} = \begin{cases} \frac{1}{2q}(3\sigma_{ij} - p) & i = j \\ \frac{3\sigma_{ij}}{q} & i \neq j \end{cases} \qquad p = \frac{1}{3}\sum \sigma_{ii} \tag{11}$$

$$\frac{\partial g}{\partial \sigma_{ij}} = \frac{\sin\left(\beta\frac{\pi}{6} - \frac{1}{3}\arccos(\gamma X)\right)}{\sqrt{1-(\gamma X)^2}}\frac{9}{2}\gamma g^2 \frac{1}{q^3}\left(\frac{\partial J_3}{\partial \sigma_{ij}} - \frac{3}{q}\frac{\partial q}{\partial \sigma_{ij}}J_3\right) \tag{12}$$

Special care is to be taken in correspondence of corners ($\gamma = 1\,; X = \pm 1$), as the normal to the yield surface has an undetermined direction.

For the second case, a simple discretization scheme is used, according to the following:

$$\frac{\partial F}{\partial \sigma_{ij}} = \frac{F(\sigma_{ij} + \Delta\sigma_{ij}) - F(\sigma_{ij} - \Delta\sigma_{ij})}{2 \cdot \Delta\sigma_{ij}} \tag{13}$$

The advantage of this scheme is that it is of general validity, being applicable to any yield surface *F* formulation.

5 MODEL CALIBRATION AND VERIFICATION

The model (4) together with the functions (5) and (6) needs the three parameters ε_{th}, a, b to be identified from experimental data. The threshold strain is obtained directly from the plots in Figure 1-3. The parameters *a* and *b* can be easily determined as well from the same by plotting the ratio of the torsion to tension curve as function of the true plastic strain and by using an error minimization technique to find the optimum values. So the identification of the three parameters can be obtained directly from fitting of experimental data. By using this procedure for the steels under study, the following parameter values are obtained (Table 1).

Table 1: parameters for the yielding surface model

	ε_{th}	*a*	*b*
Grade 65	0.16	4.2	0.15
Grade 52	0.0	15	0.25
33MnB5	0.025	5	0.45

The ratio *R* of torsion to tension curve may be written in terms of (4) by putting in the function *g(X)* the value *X=1* for tension and *X=0* for torsion, obtaining:

$$R = \frac{g0}{g1} = \frac{g(X=0)}{g(X=1))} \tag{10}$$

The yield surface model (4) response in terms of ratio *R*, fitted by the parameters value of Table 1, is represented in Figures 5-7 for the three steels. It can be seen that the simple exponential formulation proposed is able to reproduce with good accuracy the evolution of the ratio *R*. It is to be noted that the above parameters describe the distortion of the yield surface section in the deviatoric plane, which evolves from the initial von Mises round section toward a polygonal section. This may suggest a possible link with the strain fracture limits which depend on the *J3* invariant too [27].

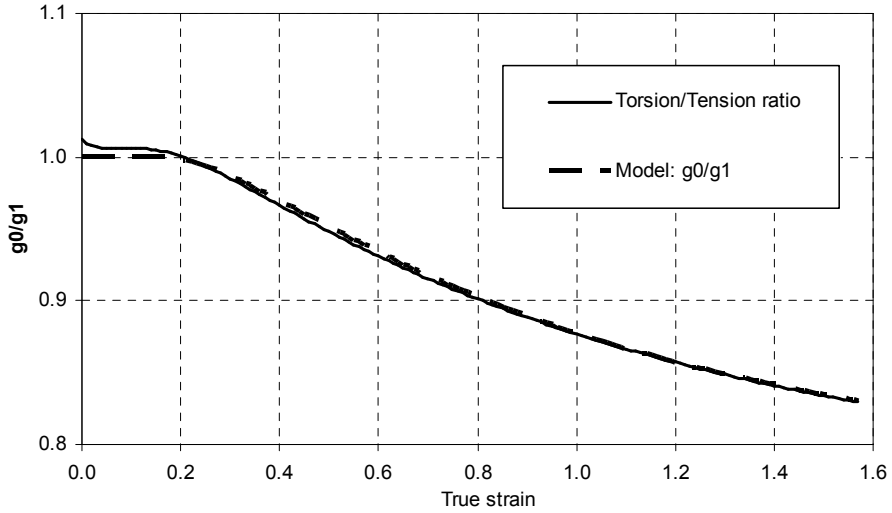

Figure 4: *Grade 65*, comparison between experimental tests and model fitting

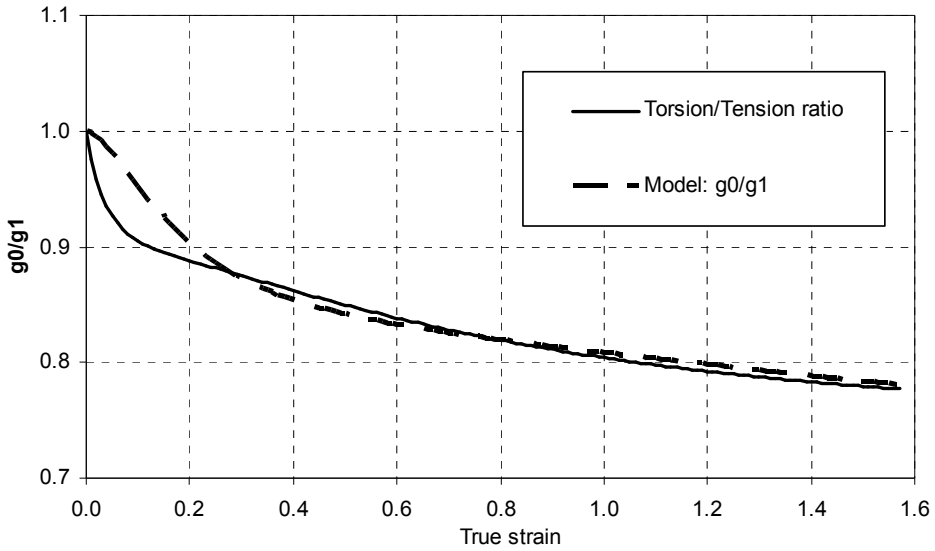

Figure 5: *Grade 52*, comparison between experimental tests and model fitting

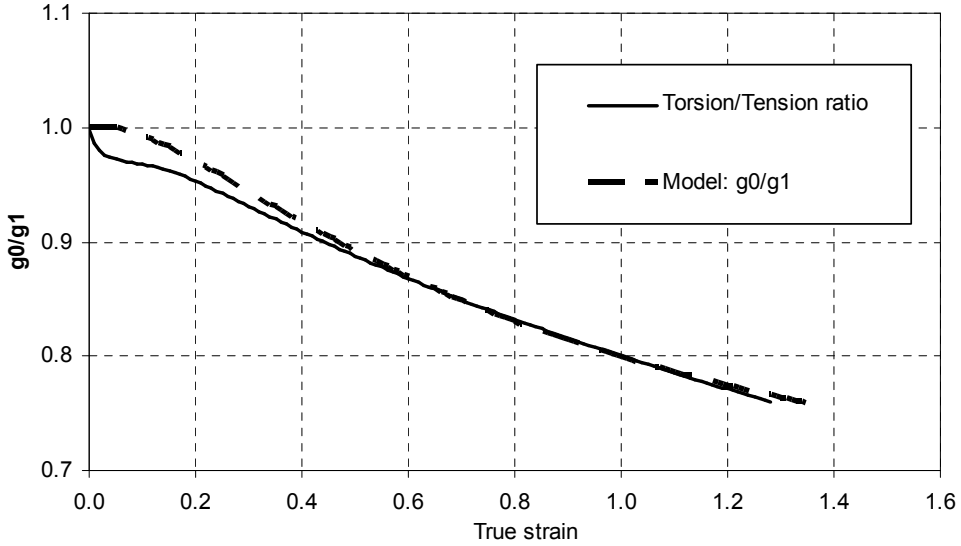

Figure 6: *33MnB5*, comparison between experimental tests and model fitting

The tensile and torsion tests have been next modeled by means of Finite Elements. The commercial general purpose code *Msc.Marc*, release 2010, has been used together with dedicated user routines for the yield surface and its derivatives calculation. The experimental tests have been modeled by using an axisymmetric scheme.

For tensile tests modeling, standard four nodes, full integration axisymmetric elements have been used, while for torsion test modeling a special axisymmetric element available in the *Msc.Marc* library has been used [28] which includes an extra degree of freedom at nodes for twist and is also suitable for large displacement and finite plasticity options. Each test has been modeled and the Finite Element response has been extracted and plotted in terms of remote global quantities, such as load vs. clip gauge displacement for tensile tests and torque vs. rotation for torsion tests. The comparison between the experimental curves and the

calculated ones is shown in Figures 7-9. It can be observed a very good match in all cases, that would be impossible by using the standard von Mises criterion.

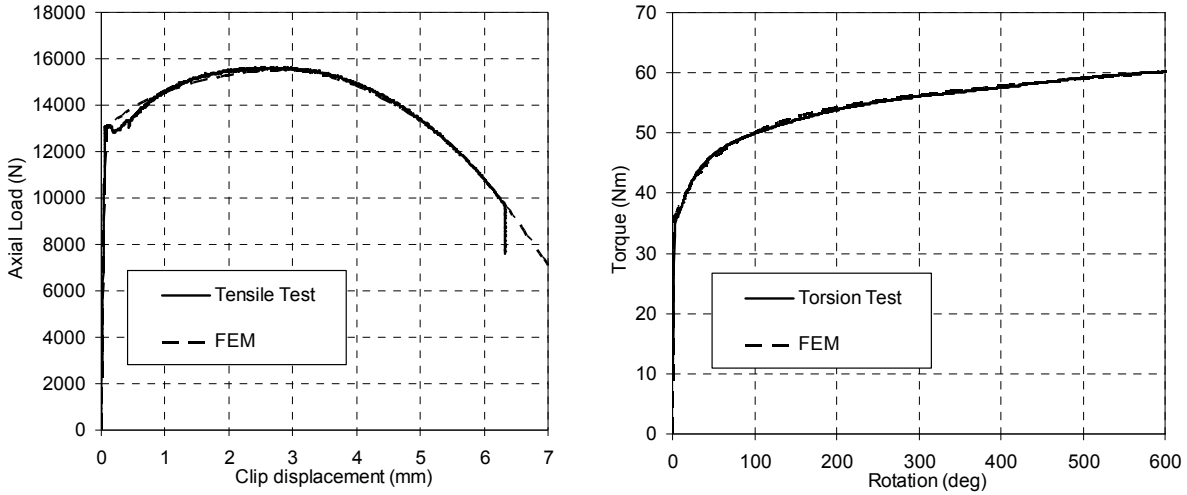

Figure 7: *Grade 65*, global response comparison between tensile (left) and torsion (right) experimental tests and finite element model incorporating the new yield criterion

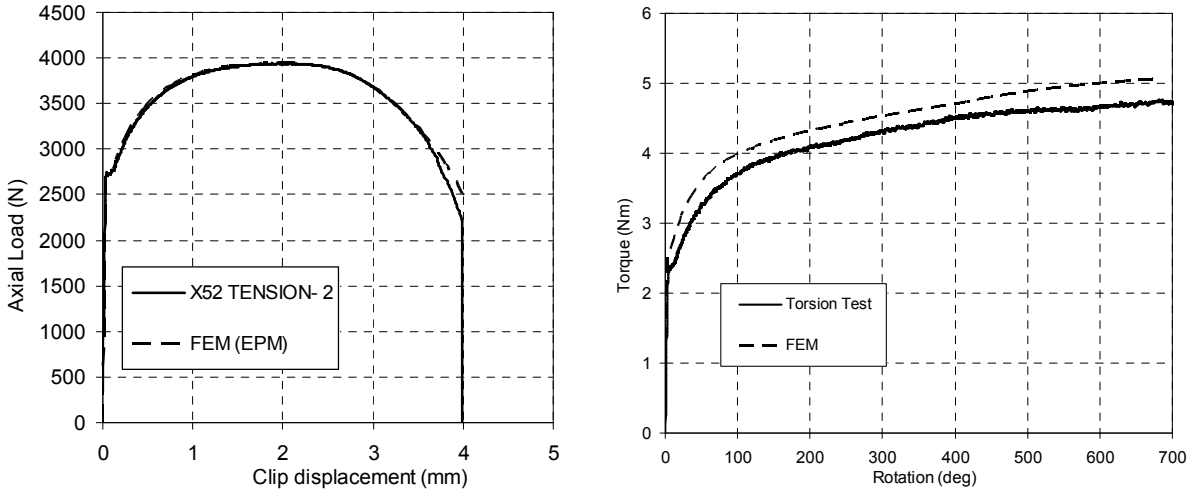

Figure 8: *Grade 52*, global response comparison between tensile (left) and torsion (right) experimental tests and finite element model incorporating the new yield criterion

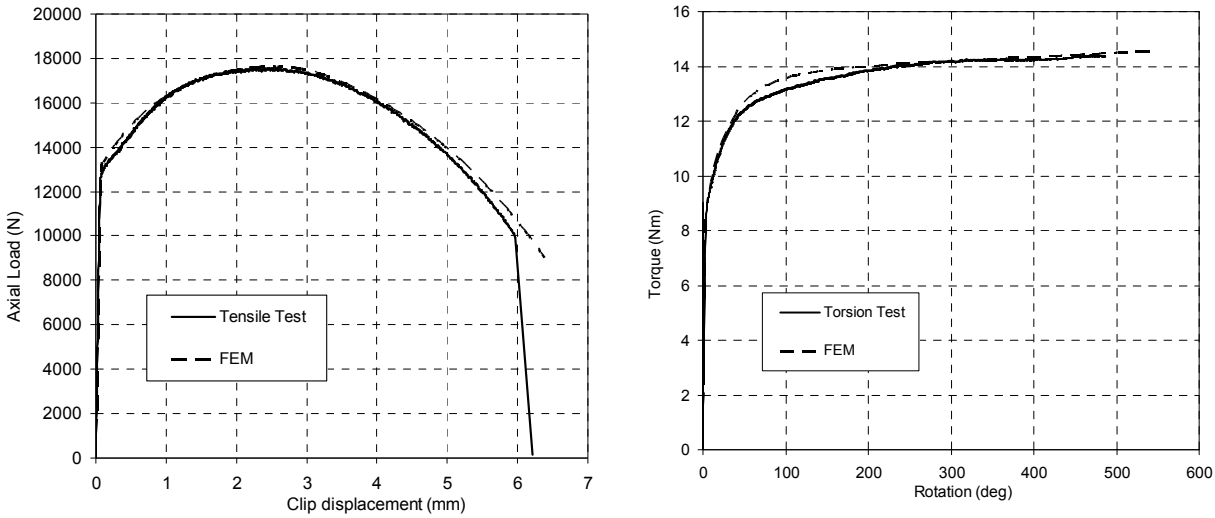

Figure 9: *33MnB5*, global response comparison between tensile (left) and torsion (right) experimental tests and finite element model incorporating the new yield criterion

6 CONCLUSIONS

Starting from a set of conventional experimental tests on steels, namely tensile and torsion tests up to fracture, a general yield function has been developed based on a well established framework, including beside the *J2* invariant also the *J3* one. The proposed yield function has been embedded into a general purpose Finite Element code and tested against experimental results to verify the function accuracy. The distortion of the yield surface section in the deviatoric plane, which evolves from the initial von Mises round section toward a polygonal section, may suggest a possible link with the strain fracture limits which depend on the *J3* invariant too.

ACKNOWLEDGMENTS

Part of the experimental tests were carried out with a financial grant of the Research Programme of the Research Fund for Coal and Steel, Contract N. RFSR-CT-2011-00029.

REFERENCES

[1] Lode W. ,Versuche über den Einfluß der mittleren Hauptspannung auf das Fließen der Metalle Eisen Kupfer und Nickel, Zeitschrift für Physik, Vol.36, no. 11-12, pp. 913–939, 1926.
[2] Ros M., Eichinger A., Versuche zur Klaerung der Frage der Bruchgefahr III, Metalle, EMPA-Bericht Nr. 34, 1929.
[3] Taylor G.I., Quinney H., *The plastic distortion of metals*, Philosophical Transactions of the Royal Society London A, vol. 230, no. 681-693, pp. 323-352, 1932.
[4] Mendelson A., Plasticity: Theory and Application, MacMillian Series in Applied Mechanics, ed. Landis F., The MacMillian Company, New York, p. 92, p.109, 1968.
[5] Spitzig W.A., Sober R.J., Richmond O., *Pressure dependence of yielding and associated volume expansion in tempered martensite*. Acta Metallurgica, vol. 23, no. 7, pp.885–893, 1975.
[6] Richmond O., Spitzig W.A., Pressure dependence and dilatancy of plastic flow. In: Theoretical

and Applied Mechanics, 15th International Congress of Theoretical and Applied Mechanics, Toronto, Canada. North-Holland Publ. Co., Amsterdam, The Netherlands, pp. 377–386, 1980.
[7] Wilson C.D., *A critical reexamination of classical metal plasticity*. Journal of Applied Mechanics, Transactions ASME, vol.69, no.1, pp. 63–68, 2002.
[8] Brunig M., *Numerical simulation of the large elastic–plastic deformation behavior of hydrostatic stress-sensitive solids*. Int. Jou. of Plasticity, vol. 15, no. 11, pp.1237–1264, 1999.
[9] Kuroda M., *A phenomenological plasticity model accounting for hydrostatic stress-sensitivity and vertex-type of effect*, Mechanics of Materials, vol.36, no. 3, pp. 285-297, 2004.
[10] Prager W., *Strain Hardening Under Combined Stresses*, Jou. of Applied Physics, vol. 16, no. 12, pp.837-840.
[11] Ohashi Y., Tokuda M., *Precise measurement of plastic behaviour of mild steel tubular specimens subjected to combined torsion and axial force*, Journal of the Mechanics and Physics of Solids, Vol. 21, no. 4, pp. 241- 261, 1973.
[12] Miller M.P., McDowell D.L., *Modeling large strain multiaxial effects in FCC polycrystals*, International Journal of Plasticity, vol. 12, no. 7, pp.875-902, 1992.
[13] Brunig M., Berger S., Obrecht H., *Numerical simulation of the localization behavior of hydrostatic-stress-sensitive metals*, Int. Jou. of Mech. Sci., vol. 42, no. 11, pp. 2147-2166, 2000.
[14] Yang F., Sun Q., Hu W., *Yield criterions of metal plasticity in different stress states*, Acta Metallurgica Sinica (English Letters), vol.22, no.2, pp. 123-130, 2009.
[15] Bai Y., Wierzbicki T., *A new model of metal plasticity and fracture with pressure and Lode dependence*, Int. Jou. of Plast., vol. 24, no. 6, pp.1071-1096, 2008.
[16] Gao X., Zhang T., Zhou J., Graham S. M., Hayden M., Roe C., *On stress-state dependent plasticity modeling: Significance of the hydrostatic stress, the third invariant of stress deviator and the non-associated flow rule*, Int. Jou. of Plast., vol. 27, no. 2, pp. 217-231, 2011.
[17] Hu W., Wang Z.R., *Multiple-factor dependence of the yielding behavior to isotropic ductile materials,* Computational Materials Science, vol.32, no.1, pp.31-46, 2005.
[18] Yu, M.H., 2002. *Advances in strength theories for materials under complex stress state in the 20th Century*, Appl. Mech. Rev., 55, no 3.
[19] Bardet J.P., *Lode Dependences for Isotropic Pressure-Sensitive Elastoplastic Materials*, Jou. of Applied Mech., vol. 57, no. 3, pp. 498-506, 1990.
[20] Menétrey P., Willam K.J., *Triaxial failure criterion for concrete and its generalization*. ACI Structural Journal, vol. 92, pp.311–318, 1995.
[21] Bigoni D., Piccolroaz A., Yield criteria for quasibrittle and frictional materials, International Journal of Solids and Structures, vol.41, pp. 2855-2878 , 2004.
[22] Bufalini A., Morana R., Nice P.I., Nasvik H., Kjørholt H., Bailey B.M., Adam M.K., Jiral D.G., Ross R.C., Smith B., Ueda M., Ohe T., *Evaluation of Mechanical Performance and Stress-Corrosion-Cracking Resistance of Post Expanded Carbon Steel and CRA Casing Grades*. SPE 133382, SPE ATCE, Florence, 2010.
[23] Broggiato G.B., Cortese L ., *Sviluppo di un sistema di prova biassiale per la caratterizzazione del legame elasto-plastico e del danneggiamento duttile*. XXXVII AIAS, Rome, 2008.
[24] Ling Y., *Uniaxial True Stress-Strain after Necking*, AMP Jou. of Tech., vol. 5, pp.37- 48, 1996.
[25] Coppola T., Demofonti G., Mannucci G., *Numerical-Experimental Procedures To Identify The Ductile Fracture Strain Limits In Pipeline Steel*, XIX ISOPE Conference, Strain-based Design Symposium, Vol. IV, TPC 761, Osaka, 2009.
[26] McClintock F.A., Argon A.S., Mechanical behaviour of materials. Addison-Wesley Publishing Company, Boston, 1966.
[27] Coppola T., Cortese L., Folgarait P., *The effect of stress invariants on ductile fracture limit in steels*. Eng. Fract. Mech. 76, 1288-1302, 2009.
[28] *Msc.Marc* user manual. Release 2010. Vol. *A-D*.